JOURNAL OF Materials CHEMISTRY

Assemblies of aziridinemethanols

Peter J. J. A. Buijnsters,[a]† Martinus C. Feiters,[a] René de Gelder,[b] Peter ten Holte,[a] Roeland J. M. Nolte,[a,d] Arthur M. A. Pistorius,[c] Nico A. J. M. Sommerdijk,*[a,d] Sandy A. C. Verhaegen[a] and Binne Zwanenburg[a]

[a]*Department of Organic Chemistry, NSR Center for Molecular Structure, Design and Synthesis, University of Nijmegen, Toernooiveld 1, NL-6525 ED Nijmegen, The Netherlands. E-mail: N.Sommerdijk@tue.nl*
[b]*Department of Inorganic Chemistry, NSR Center for Molecular Structure, Design and Synthesis, University of Nijmegen, Nijmegen, The Netherlands*
[c]*Department of Biochemistry, University of Nijmegen, Nijmegen, The Netherlands*
[d]*Laboratory of Macromolecular and Organic Chemistry, Eindhoven University of Technology, Eindhoven, The Netherlands*

Received 7th August 2000, Accepted 8th November 2000
First published as an Advance Article on the web 4th January 2001

Two novel long chain aziridinemethanols (**1b, c**) are described and their molecular organisation in the bulk and self-assembling properties in aqueous dispersion are reported. The orientation of the NH hydrogen of the aziridinealcohol moiety in **1b** can be changed by introducing a methyl substituent into the rigid three-membered ring (**1c**), leading to a change in the hydrogen bonding pattern interconnecting these molecules. This change in configuration leads to marked differences in the ordering of these molecules in the solid state. Although compounds **1b** and **1c** both form highly organised structures in aqueous media and on the air–water interface, noteworthy differences are observed. Compound **1c** yields left-handed helical ribbons whereas no chiral aggregates are found for **1b**. However, the addition of 2-acetoxybenzoic acid (aspirin) to an aqueous dispersion of **1b** leads to the generation of both left- and right-handed helical structures. Under these conditions a reaction had taken place that was specific for the *ortho*-isomer of acetoxybenzoic acid.

Introduction

One of the current interests in supramolecular chemistry is the design of well-defined supramolecular architectures by programmed self-assembly of amphiphilic molecules. Surfactants designed to have specific intermolecular interactions have been reported to form highly organised aggregates including ribbons, tubes, toroids, and helical structures.[1–7] Assemblies with well-defined shapes and surfaces have been used as templates for the structuring of inorganic[8–11] and polymer composite materials[12] and as catalysts for (enantio)selective transformations in solution.[13] It is well recognised that hydrogen bonding is very important in the generation of supramolecular aggregates.[1–7,14]

As part of our studies on aziridine ring systems[15] we observed that highly ordered structures can be generated from aziridinemethanol moieties by the formation of hydrogen bonds. This is evidenced by the crystal structure of compound **1a** (Fig 1a),[15b] in which the molecules of **1a** are organised into linear arrays. *Inter*molecular hydrogen bonds are formed between the OH groups and the nitrogen atoms of neighboring molecules, while an *intra*molecular hydrogen bond between the NH group and the oxygen atom locks the aziridine methanol group into a rigid conformation in which the plane through N–C1–C2 is orthogonal to the C2–C3–O plane. We anticipated that the high degree of interconnectivity and rigidity of these molecules would offer prospects for the application of aziridinemethanols as building blocks in the generation of assemblies with organised and potentially reactive surfaces.

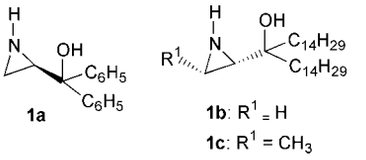

It has been demonstrated by Mathis *et al.*[16] that the configuration at the nitrogen atom of substituted aziridines can be controlled by introducing an additional substituent at the C2 position. They showed that the NH hydrogen atoms in *cis*-2,3-disubstituted aziridines have a *trans*-configuration with

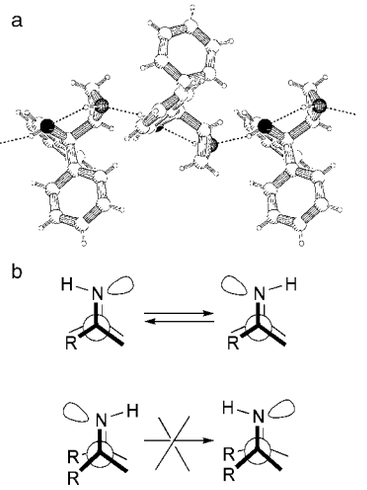

Fig. 1 (a) PLUTO drawing of the crystal structure of **1a**. (b) Newman projections of the possible configurations of an unsubstituted and a substituted aziridine ring.

†Present address: Department of Medicinal Chemistry, Janssen Research Foundation, Beerse, Belgium.

respect to the substituents. In contrast, both *cis*- and *trans*-configurations are possible in monosubstituted aziridines (Fig. 1b). Since the inversion of the nitrogen atom can be used to modify the hydrogen bonding pattern and hence the interconnectivity of these molecules, we decided to synthesize two chiral, amphiphilic, long chain aziridinemethanols **1b, c** (Scheme 1) which may be expected to show thermotropic as well as lyotropic liquid crystalline behaviour.[17,18]

In this paper we demonstrate that differences in the organisation pattern of molecules of **1b, c** in the solid state are directly linked to the configuration of the aziridine nitrogen. The molecular organisation of **1b** is dominated by a hydrogen bonding pattern similar to the one present in the crystal structure of **1a**. In the case of **1c**, a different, weaker hydrogen bonding network is present as a result of an additional substituent at the aziridine ring, and the organisation of the molecules is predominantly determined by molecular packing. When dispersed in aqueous media **1b** forms micellar fibers, whereas in dispersions of **1c** helical ribbons are observed. The addition of 2-acetoxybenzoic acid (aspirin) to aggregates of **1b**, however, induces the formation of helical structures.

Experimental

Synthesis

General. Flash column chromatography was performed on Merck silica gel 60H (0.005–0.040 mm) using a pressure of *ca.* 1.5 bar. Melting points were measured on a Reichert thermopan microscope equipped with crossed polarizers. Optical rotations were determined at 20 °C using a Perkin-Elmer automatic polarimeter, model 241. Routine FT-IR spectra were recorded using a Biorad WIN-IR FTS-25 single beam spectrometer. ^{1}H NMR and ^{13}C NMR spectra were recorded on a Bruker AC 300 (300 and 75.1 MHz) spectrometer. Mass spectra were recorded with a double-focusing VG 7070E spectrometer. Elemental analyses were determined with a Carlo Erba Instruments EA 1108 element analyser. Diethyl ether was pre-dried over potassium hydroxide, then distilled from sodium–benzophenone. Ethyl acetate and hexane were distilled under reduced pressure using a rotary evaporator.

(−)-[(2*S*)-1-Tritylaziridin-2-yl](ditetradecyl)methanol (3b). A solution of *n*-tetradecyl bromide (1.37 g, 5 mmol) in dry diethyl ether (25 ml) was added to freshly ground magnesium turnings (0.12 g, 5 mmol) in refluxing dry diethyl ether (75 ml) and this mixture was vigorously stirred for 2 h. After cooling to room temperature a solution of **2b** (0.50 g, 1.46 mmol) in dry diethyl ether (50 ml) was added dropwise. The reaction mixture was stirred overnight, quenched with saturated ammonium sulfate and subsequently the aqueous layer was extracted with ether (3 × 10 ml). After separation, the combined ether layers were washed with brine and dried over $MgSO_4$. A yellowish oil was obtained after evaporation of the solvent. Flash column chromatography (SiO_2, hexane–ethyl acetate, 20 : 1 (v/v)) yielded a colorless oil in 67% yield, which solidified on standing. Mp 35–36 °C. $[\alpha]_D^{20}$ −33.7 (*c* 1.0, EtOH). IR(KBr) 3486 (OH), 3084–3033 ($CH_{aromatic}$), 2950–2849 (CH_{alkyl}) cm^{-1}. ^{1}H NMR ($CDCl_3$) δ 7.47–7.19 (m, $C_{19}H_{15}$, 15 H), 3.07 (s, O*H*, 1 H), 1.94 (d, J = 3.2 Hz, 1 H, β-C*H*), 1.41 (dd, J = 6.5, 3.3 Hz, 1 H, α-C*H*), 1.27–1.20 (m, 52 H, 2 × $(CH_2)_{13}$), 1.10 (d, J = 6.5 Hz, 1 H, β-C*H*), 0.89 (m, 6 H, 2 × CH_3). CI-MS (*m*/*z*) 707 [M^+], 630 [$C_{44}H_{72}NO^+$], 464 [$C_{31}H_{62}NO^+$], 446 [$C_{30}H_{60}N^+$], 243 [$C_{19}H_{15}^+$]. Anal. calcd. for $C_{50}H_{77}NO$: C 84.80, H 10.96, N 1.98; found: C 85.06, H 11.44, N, 2.06%.

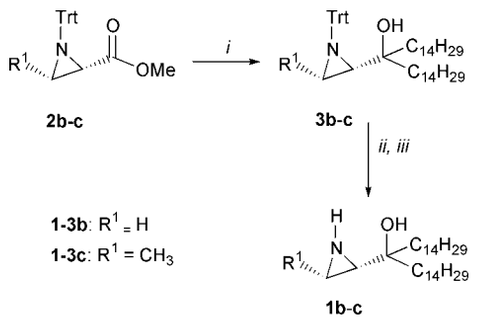

Scheme 1 *i*: $C_{14}H_{29}MgBr$–Et_2O; *ii*: MeOH–H_2O–H_2SO_4 (60 : 8 : 3, v/v/v); *iii*: Et_3N–hexane.

(+)-[(2*S*,3*S*)-1-Trityl-3-methylaziridin-2-yl](ditetradecyl)-methanol (3c). Using the same procedure as for **3b**, **3c** was obtained in 73% yield as a colourless oil starting from **2c**. $[\alpha]_D^{20}$ +22.4 (*c* 1, $CHCl_3$). IR(KBr) 3472 (OH), 3085–3020 ($CH_{aromatic}$), 2950–2552 (CH_{alkyl}) cm^{-1}. ^{1}H NMR ($CDCl_3$) δ 7.49–7.20 (m, 15 H, $C_{19}H_{15}$), 3.43 (s, 1 H, O*H*), 1.49 (d, J = 5.8 Hz, 1 H, α-C*H*), 1.32 (d, J = 6.8 Hz, 3 H, 1 × CH_3), 1.4–1.1 (m, 53 H, 2 × $(CH_2)_{13}$ and β-C*H*), 0.8 (m, 6 H, 2 × CH_3). CI-MS (*m*/*z*) 479 [$C_{32}H_{64}NO^+$], 282 [$C_{18}H_{35}NO^+$], 243 [$C_{19}H_{15}^+$], 225 [$C_{15}H_{29}O^+$], 166 [$C_{13}H_{10}^+$], 57 [$C_3H_7N^+$], 43 [$C_2H_5N^+$]. Anal. calcd. for $C_{51}H_{79}NO$: C 84.82, H 11.03, N 1.94; found: C, 84.86, H 11.00, N 1.91%.

Compound 1a. The synthesis of compound **1a** has been described previously.[15b]

(−)-[(2*S*)-Aziridin-2-yl](ditetradecyl)methanol (1b). Compound **3b** (1.40 g, 1.98 mmol) was dissolved in a mixture of MeOH, water and concentrated H_2SO_4 (60 : 8 : 3; 200 ml) by sonication for 5 min. After stirring overnight and subsequent addition of ice (50 g), the white precipitate was filtered off and successively washed with hexane (20 ml) and water (20 ml). A white solid was obtained in 67% yield. The white precipitate was dispersed in hexane and triethylamine (5 : 1; v/v, 50 ml) and the organic layer was washed with saturated ammonium sulfate solution (3 × 10 ml), dried over Na_2SO_4 and concentrated *in vacuo*. The pure compound was obtained by flash column chromatography (SiO_2, hexane–ethyl acetate, 10 : 1 (v/v)) as a white solid in 89% yield. Mp 40–41 °C. $[\alpha]_D^{20}$ −6.2 (*c* 1, EtOH). ^{1}H NMR ($CDCl_3$) δ 3.36 (s, 1 H, O*H*), 2.06 (dd, J = 6.0, 3.7 Hz, 1 H, α-C*H*), 1.69 (d, J = 6.1 Hz, 1 H, β-C*H*), 1.59 (d, J = 3.7 Hz, 1 H, β-C*H*), 1.26 (m, 53 H, N*H*, 2 × $(CH_2)_{13}$), 0.88 (m, 6 H, 2 × CH_3). ^{13}C NMR ($CDCl_3$) δ 70.8 (*C*OH), 41.2 (2 × $(CH_2)C_{13}H_{27}$), 38.9 (2 × $C_{11}H_{22}CH_2C_2H_5$), 36.2 (CH_2(NH)*C*HCOH), 32.6–30.1 (2 × $C_3H_7C_8H_{16}C_3H_7$), 24.4–23.4 (2 × $CH_2CH_2CH_2C_{11}H_{23}$, 2 × $C_{12}H_{24}CH_2CH_3$), 21.5 (CH_2(NH)*C*H), 14.8 (2 × $C_{13}H_{26}CH_3$). IR(KBr) 3600–3100 (OH, $NH_{aromatic}$), 2950–2552 (CH_{alkyl}) cm^{-1}. CI-MS (*m*/*z*) 465 [M^+], 423 [$C_{29}H_{59}O^+$], 268 [$C_{17}H_{34}NO^+$], 71 [$C_3H_5NO^+$], 42 [$C_2H_4N^+$]. Anal. calcd. for $C_{31}H_{63}NO$: C 79.93, H 13.63, N 3.01; found: C 79.82, H 13.65, N 3.09%.

(+)-[(2*S*,3*S*)-3-Methylaziridin-2-yl](ditetradecyl)methanol (1c). Using the same procedure as for **1b**, **1c** was obtained as a white solid in 35% yield, starting from **3c**. $[\alpha]_D^{20}$ +3.2 (*c* 1, $CHCl_3$). ^{1}H NMR ($CDCl_3$) δ 2.83 (s, 1 H, O*H*), 2.13 (m, 1 H, β-C*H*), 1.98 (d, J = 6.0 Hz, 1 H, α-C*H*), 1.50 (m, 4 H, 2 × COHCH_2), 1.35 (d, J = 6.0 Hz, 3 H, CH_3), 1.38–1.26 (m, 49 H, N*H*, 2 × $(CH_2)_{12}$), 0.88 (m, 6 H, 2 × CH_3). ^{13}C NMR ($CDCl_3$) δ 71.5 (quat. *C*), 42.4 (2 × $CH_2C_{13}H_{27}$), 40.7 ((CH$_3$)CH(NH)*C*H), 38.5 (2 × $C_{11}H_{22}CH_2C_2H_5$), 32.6–30.1 (2 × $C_3H_6(CH_2)_8C_3H_7$), 30.8 ((CH$_3$)*C*H(NH)CH), 24.4–23.4 (2 × $CH_2CH_2CH_2C_{11}H_{23}$, 2 × $C_{12}H_{24}CH_2CH_3$), 15.2 ((*C*H$_3$)CH(NH)CH), 14.8 (2 × $C_{13}H_{26}CH_3$). IR(KBr) 3356

(OH), 3269 (NH), 2950–2552 (CH_{alkyl}) cm^{-1}. FAB-MS (*m/z*) 480 [$M^+ + 1$], 465 [$C_{31}H_{62}NO^+$], 82 [$C_{18}H_{36}NO^+$], 58 [$C_3H_7N^+$]. Anal. calcd. for $C_{32}H_{65}NO$: C 80.09, H 13.65, N 2.92; found C 80.02, H 13.82, N 2.88%.

(+)-2{[(2*R*)-2-Acetamido-3-hydroxy-3-tetradecylheptadecyl]-oxy}benzoic acid (4). An aged (24 h) aqueous dispersion of **1b** (100 mg, 2% w/w) and 1 equivalent of aspirin (38.7 mg, 0.21 mmol) was extracted with $CHCl_3$ (3×50 ml), acidified with HCl (0.1 M, 2×50 ml) and again extracted with $CHCl_3$ (3×50 ml). After drying (Na_2SO_4) of the combined organic layers, the solvent was removed *in vacuo* and the residue (140 mg) was subjected to flash column chromatography (SiO_2, ethyl acetate), which afforded **4** as a white powder in 30% yield. Mp 59–60 °C. $[\alpha]_D^{20}$ +25.4 (*c* 2.3, $CHCl_3$). IR(KBr) 3600–3000 (C(O)OH), 3407 (OH), 3337 (NH), 2920, 2850 (CH alkyl), 1683 (C=O(OH)), 1645 (amide I), 1522 (amide II), 1254 (arom. ether) cm^{-1}. ^{1}H NMR ($CDCl_3$) δ 10.56 (s, 1 H, COO*H*), 7.79–7.75 (m, 1 H, $H_{Ph,6}$), 7.47–7.42 (m, 1 H, $H_{Ph,4}$), 6.98–6.95 (m, 1 H, $H_{Ph,5}$), 6.90–8.85 (m, 1 H, $H_{Ph,3}$) 6.08 (d, $J = 9.2$ Hz; 1 H, CHN*H*C(O)), 4.58–4.43 (m, 2 H, OCH_2CHNH), 4.35–4.30 (m, 1 H, OCH$_2$C*H*NH), 2.09 (s, 1 H, O*H*), 2.01 (s, 3 H, C(O)CH_3), 1.57 (m, 4 H, $2 \times$CH(OH)CH_2), 1.25 (m, 48 H, $2 \times$(CH_2)$_{12}$CH$_3$), 0.87 (t, $J = 6.3$ Hz, 6 H, $2 \times$(CH$_2$)$_{12}$CH_3). ^{13}C NMR ($CDCl_3$) δ 172.86 (NH*C*(O)CH$_3$), 165.5 (*C*OOH), 155.63 ($C_{Ph,2}$), 129.59 ($C_{Ph,4}$), 127.3 ($C_{Ph,6}$), 118.71 ($C_{Ph,5}$), 118.04 (HOOC$C_{Ph,1}$), 109.25 ($C_{Ph,3}$), 86.44 (*C*OH), 68.07 (O*C*H$_2$CHNH), 55.66 (OCH$_2$*C*HNH), 34.69 ($2 \times C$H$_2$C$_{13}$H$_{27}$), 30.86–22.11 ($2 \times C_{11}$H$_{22}$CH$_3$), 23.15 (NHC(O)*C*H$_3$), 13.6 ($2 \times$C$_{13}$H$_{26}$*C*H$_3$). CI-MS (*m/z*) 645 [M^+], 627 [$C_{40}H_{69}NO_4^+$], 508 [$C_{33}H_{66}NO_2^+$], 423 [$C_{29}H_{59}O^+$], 310 [$C_{22}H_{46}^+$], 121 [$C_7H_5O_2^+$], 85 [$C_4H_7NO^+$]. Anal. calcd. for $C_{40}H_{71}NO_5$: C 74.37, H 11.08, N 2.17; found: C 73.93, H 10.96, N 2.27%.

Electron microscopy

A 2% (w/v) methanolic solution (50 µl) of **1b, c** was injected in 1.0 ml of water of 60 °C adjusted to pH 3.0 with H_2SO_4. After 1 h the dispersion was cooled to room temperature and left for 2 h before EM samples were prepared. When organic counter ions were used a 2% (w/v) methanolic solution (50 µl) of **1b** (to which 1 equivalent of the organic acid had been added) was injected in 1.0 ml of water of 60 °C. After 1 h the dispersion was cooled to room temperature and left for 24 h before EM samples were prepared. Pt-shadowed samples were prepared by bringing a drop of the dispersion on to a Formvar-coated microscope grid. The excess of the dispersion was blotted off with a filter paper after 1 min and the sample was shadowed under an angle of 45° by evaporation of Pt. Negatively stained samples were prepared in an analogous manner and stained with a 1% (w/w) solution of uranyl acetate. All samples were studied with a Philips TEM201 microscope (60 kV).

Monolayer experiments

Monolayers were spread on a themostatted double barrier Riegler & Kirstein trough of dimensions 6×25 cm using a chloroform solution of the surfactant ($\sim$10 µl, 1 mg ml^{-1}) and compression was started after 10 min at a rate of 7.0 cm^2 min^{-1}. The surface pressure was measured using Wilhelmy plates and for calibration octadecanol was used. The surface of compressed monolayers was studied with a Brewster Angle Microscope (NFT BAM-1) mounted on a home built trough of dimensions 14×21 cm.

Differential scanning calorimetry (DSC)

Thermograms were recorded at 1 °C min^{-1} using a Perkin Elmer DSC7 instrument and were baseline corrected. Samples were prepared using stainless steel large volume pans.

FT-IR spectroscopy

IR samples were prepared by depositing a small amount of solid on an AgCl window and subsequently heating the sample in an oven above the melting temperature. FT-IR spectra were measured using a Mattson Cygnus 100 single beam spectrometer, equipped with a liquid nitrogen cooled narrow band MCT detector, interfaced to a microcomputer. The optical bench was continuously purged with dry nitrogen gas (20 l min^{-1}). The following acquisition parameters were used: resolution, 4 cm^{-1}; moving mirror speed, 2.53 cm s^{-1}; wavenumber range, 4000–750 cm^{-1}; number of co-added interferograms, 128. Signal to noise ratios (2000–2200 cm^{-1}) were better than 4×10^3. Data acquisition was performed using EXPERT-IR software (Mattson). For data analysis PeakFit™ v4 (Jandel Scientific Software) was used. Baselines were corrected and peak positions were determined using second derivative spectra. Curve fitting procedures were repeated several times and the quality of the fitted spectra was checked by comparing the generated spectra before and after deconvolution.

Powder diffraction experiments

Samples were prepared by placing a drop of an aggregate dispersion on a silicon wafer. The instrument was a commercial Philips X-ray powder diffractometer of the Bragg Brentano type that was optimized for measurements at low angle. The X-ray tube was ceramic with a long fine focus and gave Cu-K_α radiation (generator 40 kV, 40 mA). The goniometer had a variable divergence and antiscatter slits, with the receiving slits set at 0.1 mm. The detector was of the Peltier-cooled Si/Li type. During the measurements, the sample was mounted in a chamber the relative humidity of which could be controlled by a humidifying instrument flushed with N_2 gas.[19]

Results and discussion

Synthesis

Compounds **1b, c** were prepared starting from the methyl *N*-tritylaziridinecarboxylic acid esters **2b, c** (Scheme 1).[15a,b] The compounds **2b, c** were converted into the corresponding *N*-tritylaziridinemethanols **3b, c** using an excess of tetradecylmagnesium bromide in ether. Detritylation using 6 M sulfuric acid in methanol with sonication, followed by treatment with base and subsequent chromatography afforded the pure aziridine-2-methanols.

Characterisation of the solid state structures of long chain aziridinemethanols 1b, c

Differential scanning calorimetry (DSC) experiments showed that compound **1b** exhibits two minor phase transitions between 28 and 40 °C (not detected by polarisation microscopy or variable temperature FT-IR, *vide infra*) and a melting transition at 55 °C (onset temperature) which was also observed with polarisation microscopy. In contrast, upon heating, compound **1c** showed pronounced exo- and endothermic solid state transitions between 30 and 36 °C and a melting point at 44 °C (Fig. 2a). Between 30 and 36 °C polarisation microscopy revealed a spherulitic structure,[20] transforming first into an isotropic state and subsequently into a needle-like morphology (Fig. 2b, c). The reorganisation was accompanied by a net decrease in entropy ($\Delta S = -74 \pm 1$ kJ mol^{-1}) indicating that a more ordered structure was formed. Comparison of the melting entropies (ΔS_m) of the two compounds (Table 1) suggested that in the solid state **1c** possesses a higher degree of organisation than **1b**, both before and after the transition.

Although related long chain amino alcohols have been described to form thermotropic liquid crystalline phases,[17,18]

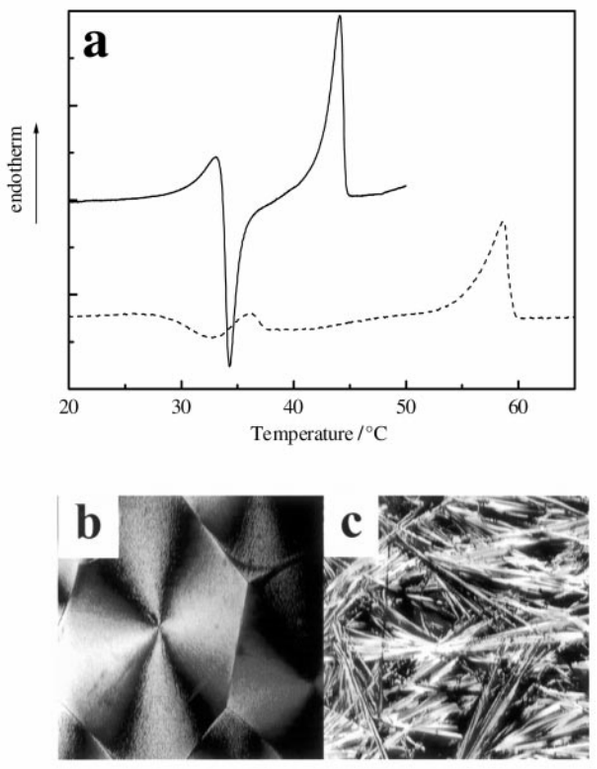

Fig. 2 (a) Thermograms of **1b** (lower trace) and **1c** (upper trace) and textures observed between crossed polarisers of the (b) spherulitic and (c) needle-like morphologies of **1c**.

no such behaviour was detected for **1b, c**. Temperature-dependent FT-IR experiments were performed on annealed films of **1b, c**, in order to obtain insight into the hydrogen bonding pattern and the packing of the alkyl chains as a function of temperature. The O–H stretching vibration of tertiary alcohols generally gives rise to absorptions in the range of 3620–3600 cm^{-1} and the N–H stretching vibration of aziridines appears in the 3360–3300 cm^{-1} region.[16,20] Hydrogen bonding is known to result in a downward frequency shift and, in general, peaks become broader as the strength of the hydrogen bonding increases.[21] The position of the CH_2 deformation band can be used to assess the organisation of the hydrocarbon chains. *gauche* Conformations give rise to a band at low wavenumbers ($\sim$1463 cm^{-1}) whereas a highly packed all-*trans* state leads to a vibration at 1471 cm^{-1}.[22]

FT-IR spectra of **1b**, recorded at different temperatures, revealed a very broad band between 3600 and 3100 cm^{-1} (Fig. 3a). This indicates a strong hydrogen bonded network[22] which continued to exist until the melting point was reached at 59 °C (peak temperature, Fig. 2a). The spectrum of **1b** in this region was nearly identical to that of **1a**, suggesting that both compounds have a similar hydrogen bonding pattern. In such a pattern the alkyl chains are placed, alternately, above and below the plane of the hydrogen bonds, giving rise to an interdigitated solid state structure (Fig. 4a). The position of the CH_2 deformation band (1468 cm^{-1}) indicated the presence of *trans* conformations in the alkyl chains, but excluded an all-*trans* conformation.[23] At 55 °C (onset temperature, Fig. 2a) this band started to shift to lower wavenumbers (1468–1465 cm^{-1}, Fig. 3e), reflecting the increase in the number of *gauche* conformations associated with the melting of the alkyl chains.[23] This suggests that in the case of **1b** at the melting point the disordering of the hydrocarbon chains precedes the breaking of the hydrogen bonds.

FT-IR spectra of **1c**, recorded between 20 and 30 °C, revealed two bands between 3600 and 3100 cm^{-1} after deconvolution (Fig. 3b, c). The broad band at 3356 cm^{-1} can be ascribed to a polymeric hydrogen bonded structure involving the hydroxy groups,[24] whereas the sharper amine stretching vibration at 3269 cm^{-1} corresponds to an intermolecular NH–OH hydrogen bond.[25] From the position of the CH_2 deformation band (1468 cm^{-1}) it can be deduced that in this temperature window the alkyl chains are not in a close-packed arrangement (Fig. 3e). Based on these data, in conjunction with the fact that the amine hydrogen atom is oriented *trans* with respect to the substituents,[16] we propose a molecular organisation in which the alkyl chains again are localised alternately above and below the plane of the hydrogen bonds, as depicted schematically in Fig. 4b.

Variable temperature FT-IR revealed that upon heating at 23 °C the alkyl chains of **1c** gradually start to become disordered (*i.e.* start to melt, Fig. 3e), until at 33 °C a rearrangement of the hydrogen bonding pattern occurred as was evident from the disappearance of the O–H and N–H vibrations at 3356 and 3269 cm^{-1} and the concomitant appearance of 4 new bands (Fig. 3b, d). The two new O–H vibrations at 3539 and 3470 cm^{-1} can be ascribed to an alcohol dimer[26] and an intramolecular hydrogen bond between the hydroxy group and the nitrogen atom,[22] respectively. The appearance of two N–H stretching bands at 3264 and 3214 cm^{-1} indicates that the amine hydrogen atom is involved in both a weak *intra*molecular and a strong *inter*molecular H-bond, respectively.[22,25,27] This proposed reorganisation was also supported by the fact that the packing of the alkyl chains increased upon heating as was evidenced by the shift of the CH_2 deformation band, going from 1468 to 1471 cm^{-1} (Fig. 3e), indicating that above 35 °C the alkyl chains adopt an all-*trans* conformation.[23] Hence from the DSC and IR data we conclude that the reordering of the hydrogen bonding network leads to a higher degree of organisation of the molecules and imposes an all-*trans* conformation upon the alkyl chains. We propose that above the transition temperature the molecules of **1c** have *intra*molecular H-bonds between the OH and the nitrogen atom and are organised in arrays held together by *inter*-molecular hydrogen bonds between the NH hydrogen atom and the neighboring OH group. In addition inter-array hydrogen bonds (alcohol dimers and NH–N hydrogen bonds, see Fig. 4c) further enhance the ordering of the molecules, resulting in a tight packing that forces the alkyl chains to adopt an all-*trans* conformation.[28] It should be noted that in this scenario while going through the isotropic state a conversion takes place to a state in which the alkyl chains are no longer interdigitating, but all become localised on the same side of the plane through the hydrogen bonds.

Based on the molecular requirements formulated by Jeffrey[17] and Van Doren *et al.*,[18] we expected compounds **1b, c** to show liquid crystalline behaviour. Jeffrey[17] has suggested that in the liquid crystalline phase the weaker van der Waals interactions are broken while the stronger hydrogen bonds remain intact, and that at the liquid crystalline-to-isotropic transition the hydrogen bonded structure breaks down. In contrast to this model, Van Doren *et al.*[18] proposed that the melting point is determined by the breaking up of the network of hydrogen

Table 1 Data derived from calorimetric experiments

	$K_1 \rightarrow K_2$	ΔH_K/kJ mol^{-1}	ΔS_m/J mol^{-1} K^{-1}	K→I	ΔH_m/kJ mol^{-1}	ΔS_m/J mol^{-1} K^{-1}
1b	Not observed	—	—	59.9	33.5	101
1c	30–35 °C	−23.1	−74	44.1 °C	61.3	193

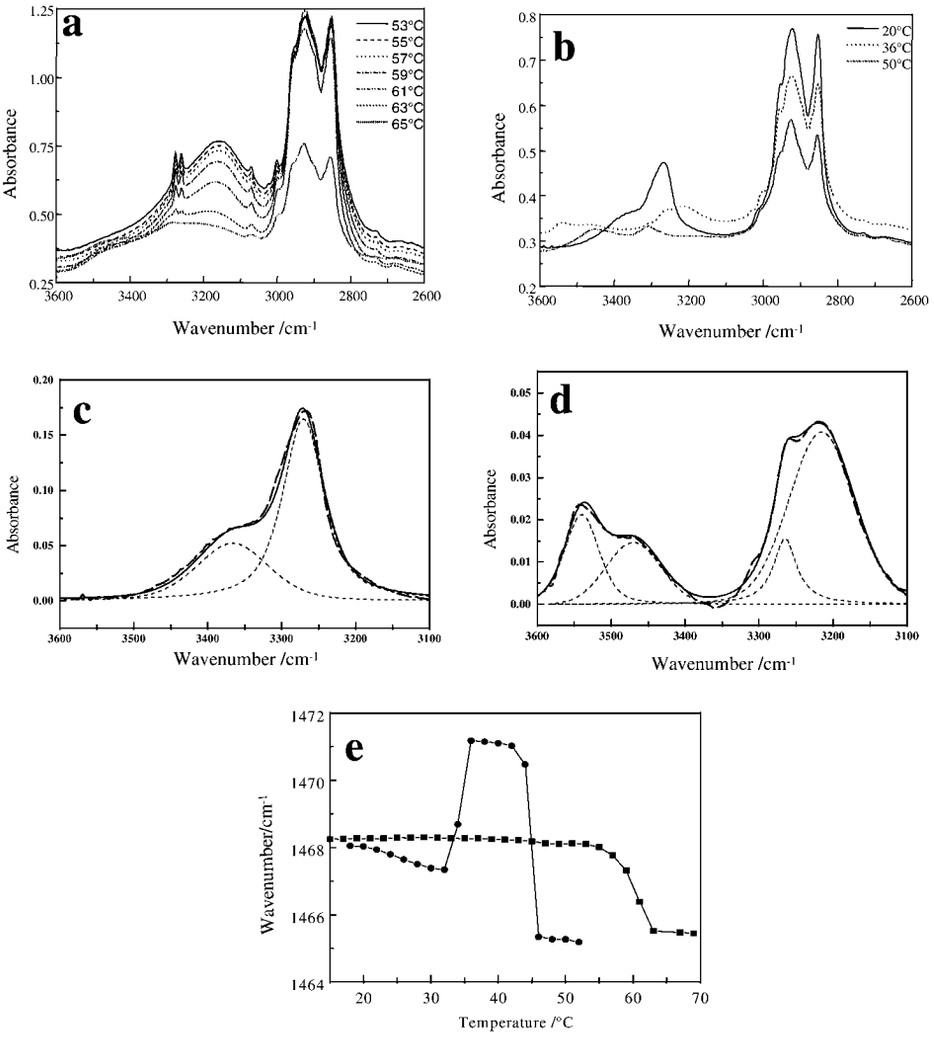

Fig. 3 Variable temperature FT-IR spectra of annealed films of (a) **1b** and (b) **1c**. Overlay of experimental and fitted FT-IR spectra of **1c** at (c) 20 °C and (d) 36 °C. (e) Temperature dependence of the position of the CH_2 deformation band in the FT-IR spectra of (■) **1b** and (●) **1c**.

bonds. Upon entering the liquid crystalline phase molecules are held together by lateral cohesive forces, which break up when at the clearing point an isotropic liquid is formed.

In the case of **1b** the hydrogen bonding network is strong enough to maintain an ordered arrangement in which melting of the alkyl chains is inhibited until a temperature of 55 °C is reached. At this temperature the hydrogen bonding arrangement weakens and the system enters the isotropic state at 59 °C. In contrast, the weaker hydrogen bonding pattern in films of **1c** apparently can not prevent the molecules from rearranging already at 23 °C. The consequent reordering of the hydrogen bonds leads to a much more efficient packing of the alkyl chains which subsequently prevents the formation of a mesophase until the melting point is reached. However, in contrast to **1b**, for **1c** the breaking of the hydrogen bonds and the melting of the alkyl chains occur simultaneously.

Aggregation behaviour of aziridinemethanol surfactants

Compounds **1b, c** did not dissolve in water of neutral or basic pH. Aqueous dispersions (0.1%; w/w), therefore, were prepared by injecting a 2.0% (w/v) methanolic solution of **1** into water of 60 °C adjusted to pH 3.0.[29] Transmission electron microscopy demonstrated that both **1b** and **1c** formed vesicles with diameters between 75 and 300 nm (not shown). Upon standing, dispersions of **1b** were transformed into fibers with diameters of approximately 5 nm and lengths of several micrometres (Fig. 5A). After ageing for several days at room temperature, vesicles of **1c** were transformed into ribbon-like bilayer structures, which rolled up to form right-handed helical ribbons with lengths > 10 μm (Fig. 5B).

Powder diffraction patterns of cast films of aged 0.1% (w/w) dispersions of compounds **1b** and **1c** revealed a repetitive distance of 40.6 and 41.6 ± 0.2 Å, respectively, indicating that the aggregates consisted of intercalated bilayers. Different levels of relative humidity (0, 50 and 90%) had no effect on the bilayer periodicity of these films, indicating that no water molecules are bound to the head groups.

Monolayer experiments

In order to obtain information about the ordering of the molecules in the aggregates, surface pressure–surface area (π–A) isotherms of **1b, c** were recorded on an aqueous sub-phase adjusted to pH 3.0 (Fig. 6A). Both isotherms showed a plateau representing the coexistence of two phases during the transition of a liquid expanded (LE) to a liquid condensed (LC) phase. Brewster angle microscopy (BAM)[30] on the monolayers of **1b** revealed that in the LE–LC coexistence phase two-dimensional dendritic solid-like domains were formed with diameters of approximately 300 μm (Fig. 6A, inset), whereas no domains were observed in the plateau region of **1c**.[31] The occupied area per molecule before and after this transition suggested that the head groups of both compounds rearrange going from a parallel to a perpendicular orientation with respect to the interface (Fig. 6B).

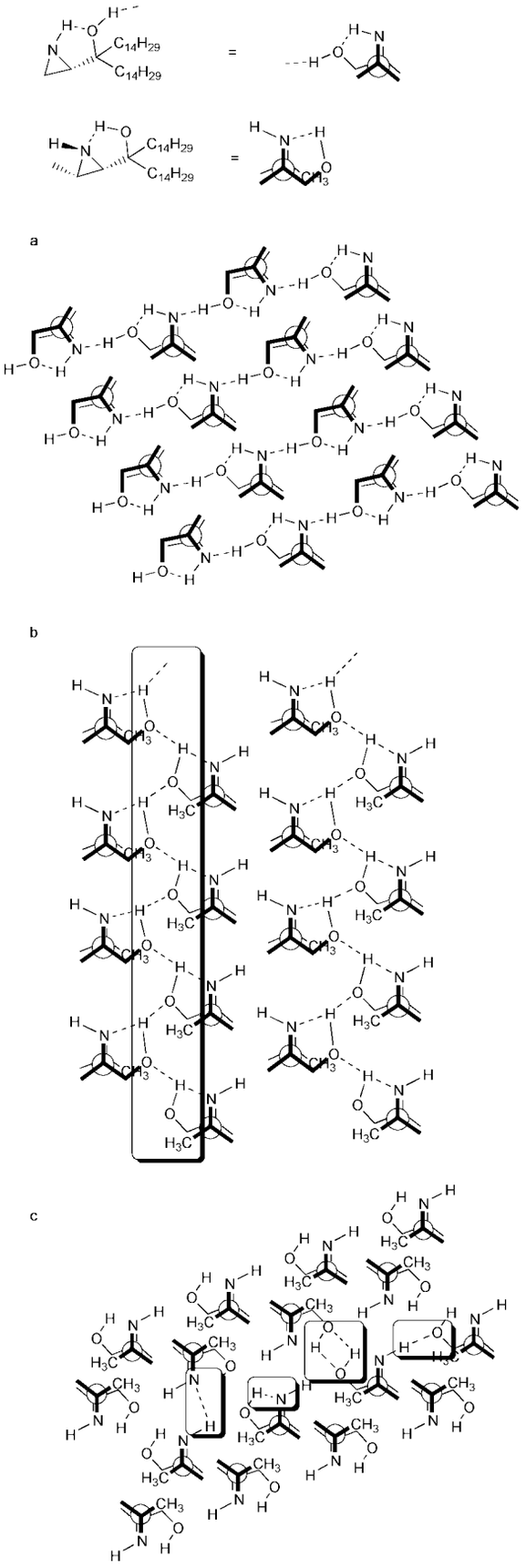

Fig. 4 Schematic representation of the proposed solid state structure of (a) **1b** and (b) **1c** at 20 °C; (c) **1c** at 36 °C.

The high collapse pressure observed for monolayers of **1b** ($\pi = 70$ mN m^{-1}) indicates that this compound forms a rigid film. It appears that specific intermolecular interactions between the head groups of **1b** are responsible for the formation of domains on the microscopic scale. Remarkably, this also results in a higher molecular area per molecule for surfactant **1b** compared to **1c**. Apparently, the methyl substituent of **1c** prevents such a highly organised structure and enables a close packing of the molecules at the air–water interface governed by van der Waals forces, but leads to films of low stability. The fact that compound **1c** forms more densely packed monolayers compared to those of **1b** is in line with the difference in ability of these compounds to form helical aggregates in aqueous dispersions.

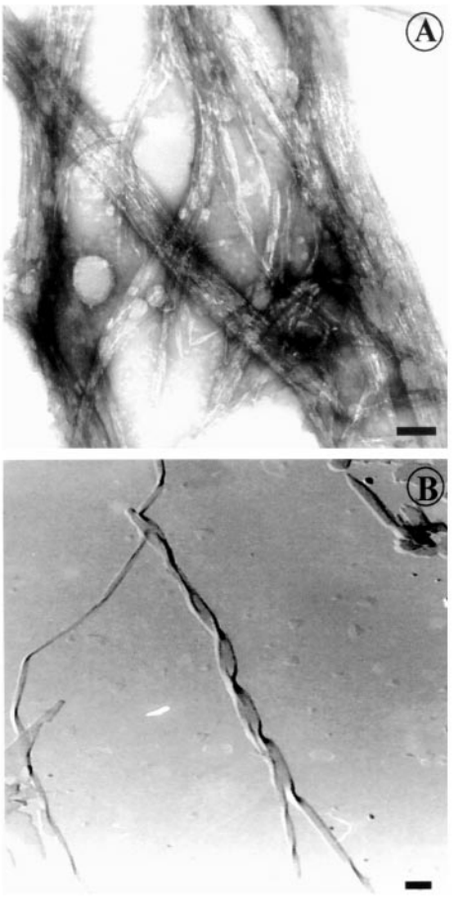

Fig. 5 Transmission electron micrographs taken after 24 h from 0.1% (w/w) dispersions of (A) **1b** (negative staining) and (B) **1c** (platinum shadow) at pH 3.0, bars represent 50 nm.

Reaction with aspirin

In the course of our efforts to fine-tune the molecular packing and thereby the morphology of the aggregates,[32] we attempted to induce the formation of chiral aggregates through the addition of salicylate ions following procedures described by Hoffmann and Ebert,[33] and by Saikaigudin *et al.*[34] This experiment, however, was not successful and only ill-defined aggregates were observed.[35] However, when a methanolic solution of **1b** and 2-acetoxybenzoic acid (aspirin) was injected into water at 60 °C, electron microscopy revealed the formation of helical structures (Fig. 7a, b). Although enantiopure (*S*)-**1b** was used in all experiments, remarkably, both left- and right-handed helices were generated. Analysis of the dispersion showed that approximately 30% of **1b** had been converted into **4** (Scheme 2). This suggests that under the action of aspirin the aziridine ring of **1b** was activated by acylation of the aziridine nitrogen atom,[15c] and subsequently opened in a regioselective manner by nucleophilic attack of the salicylate.

^{1}H NMR investigation revealed that reaction of **1b** and aspirin in CD_3OD indeed leads to the acylation of the aziridine. although at this stage no ring opening was observed. Only after

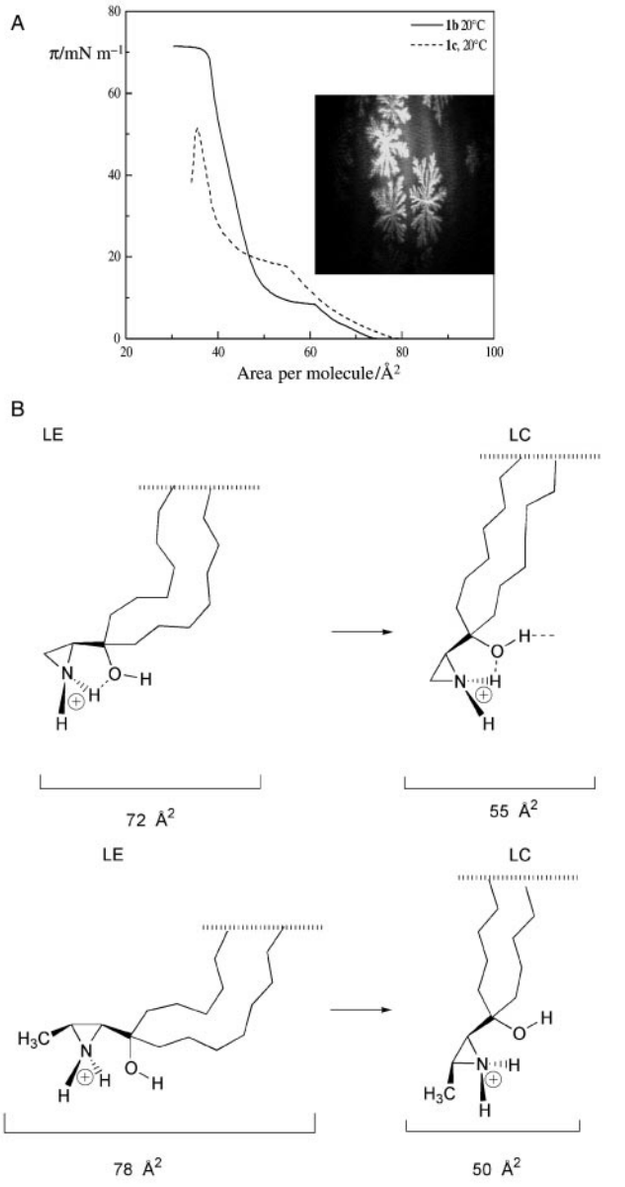

Fig. 6 (A) Langmuir isotherms of **1b** and **1c** recorded on an aqueous sub-phase of pH 3.0 at 25 °C. Inset: Brewster angle micrograph of a surface monolayer of **1b** ($\pi = 3.0$ mN m^{-1}, spot diameter 600 μm), at 15 °C and pH 3.0. (B) Proposed orientations of the head groups of **1b** (top) and **1c** (bottom) at the air–water interface in the liquid expanded (LE, left) and liquid condensed phase (LC, right).

transfer of the methanolic reaction mixture to an aqueous medium is compound **4** formed, which suggests that aggregation plays an important role in the nucleophilic ring opening by salicylic acid.

Remarkably, the reaction of **1b** was specific for aspirin. *No reaction was observed upon addition of 3- or 4-acetoxybenzoic acid to methanolic solutions of **1b*** and no distinct aggregate morphologies could be detected in aqueous dispersions of these mixtures. We propose that the reaction proceeds *via* acylation of the alcohol which, due to the rigidity of the aziridinemethanol head group and the preorganisation of the molecules in the aggregate can only occur in the case of 2-acetoxybenzoic acid. Subsequent acyl transfer from the hydroxy group to the aziridine nitrogen then may lead to activation and opening of the aziridine ring. In order to unravel the origin of helix formation it was attempted to generate these structures by dispersion of **4**, or mixtures of **4** and different amounts of **1b**, in water. This did not, however, lead to the formation of helical aggregates. Rod-like structures were observed instead for pure

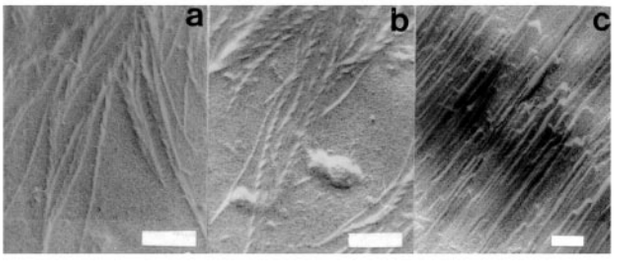

Fig. 7 Electron micrographs taken from 0.1% dispersions of **1b** and **2** in water (platinum shadowing, bars represent 250 nm). (a) Left-handed and (b) right-handed helices from **1b** and aspirin; (c) rod-like structures from **2**.

4 (Fig. 7c), whereas in dispersions of mixtures containing different ratios of **1b** and **4** no distinct morphologies could be detected. The role of (unreacted) aspirin was further investigated by adding this compound to aqueous dispersions of mixtures containing different amounts of **1b** and by injecting methanolic solutions of mixtures of **1b** and **4** into aqueous solutions of aspirin. Helix formation was not observed in any of these cases, leaving the precise effect of aspirin as yet unexplained.

Conclusions

The experiments described above demonstrate that molecules containing an aziridinemethanol moiety can form highly organised structures. The rigid, specific and strong hydrogen bonding pattern of **1b**, similar to that of **1a**, dominates the organisation of these molecules in the solid state and prevents

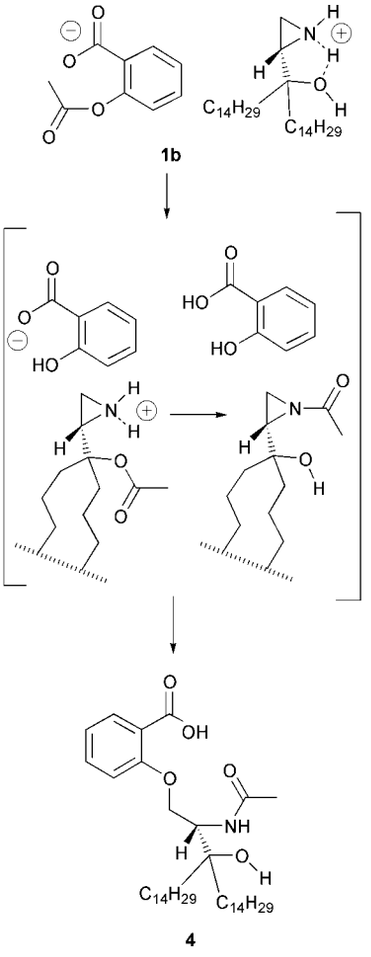

Scheme 2

the molecules from displaying thermotropic liquid crystalline behaviour.

The interconnectivity of these molecules can be disrupted by the introduction of an additional methyl substituent at the aziridine ring. This leads to a change in the configuration of the NH hydrogen atom (*trans* with respect to the substituents) and consequently to a change in the hydrogen bonding pattern of the aziridinemethanol moieties. The hydrogen bonding network of **1c** is not as rigid and strong as that of **1b** and therefore the molecules reorganise into a more stable structure when the compound is heated to the point where the alkyl chains start to melt. In this structure it is the efficient packing of the alkyl chains rather than the hydrogen bonding pattern that keeps the molecules in the solid state until the melting point is reached at 45 °C.

We have demonstrated that the introduction of the methyl substituent has a profound effect on the aggregation behaviour of the molecules in water and at the air–water interface. The specific intermolecular interactions of the head groups of **1b** lead to a highly ordered monolayer, *i.e.* the formation of two-dimensional crystalline domains. However, this rigid orientation of the head groups prevents the close packing of the molecules and hence the expression of molecular chirality in the aggregates. In contrast to that of compound **1b**, the organisation of **1c** is predominantly determined by the close packing of molecules, resulting in the expression of chirality at the supramolecular level. Our experiments show that it is possible to fine-tune the aggregate morphology of **1b** by the addition of aspirin. The specific nature of this reaction is most probably related to the rigid conformation of the head group, although the helix formation remains as yet unexplained.

Acknowledgements

The authors wish to thank F. J. Dommerholt for the kind donation of compound **1a**, H. P. M. Geurts for his assistance in performing electron microscopy experiments, A. M. Roelofsen, for performing the Langmuir film balance studies, D. S. J. van der Gaast (NIOZ, Netherlands Institute for Sea Research) for assistance with the powder diffraction experiments and L.Thijs and G. J. F Chittenden for fruitful discussions.

References

1 (*a*) J. H. Fuhrhop and W. Helfrich, *Chem. Rev.*, 1993, **93**, 1565 and references cited; (*b*) D. A. Frankel and D. F. O'Brien, *J. Am. Chem. Soc.*, 1994, **116**, 10057.
2 (*a*) N. Nakashima, S. Asakuma and T. Kunitake, *J. Am. Chem. Soc.*, 1985, **107**, 509; (*b*) T. Kunitake, J.-M. Kim and Y. Ishikawa, *J. Chem. Soc., Perkin Trans. 2*, 1991, 885; (*c*) T. Imae, Y. Takahashi and H. Muramatsu, *J. Am. Chem. Soc.*, 1992, **114**, 3414.
3 (*a*) H. Yanagawa, Y. Ogawa, H. Furuta and K. Tsuno, *Chem. Lett.*, 1988, 269; (*b*) H. Yanagawa, Y. Ogawa, H. Furuta and K. Tsuno, *J. Am. Chem. Soc.*, 1989, **111**, 4567.
4 (*a*) D. G. Rodes, S. L. Blechner, P. Yager and P. E. Schoen, *Chem. Phys. Lipids*, 1988, **49**, 39; (*b*) J. M. Schnur, *Science*, 1993, **262**, 1669; (*c*) J. M. Schnur, B. R. Ratna, J. V. Selinger, A. Singh, G. Jyothi and K. R. K. Easwaran, *Science*, 1994, **264**, 945.
5 (*a*) F. Giulieri, J. G. Riess and M. P. Krafft, *Angew. Chem.*, 1994, **106**, 1583; (*b*) F. Giulieri, F. Guillod, J. Greiner, M. P. Krafft and J. G. Riess, *Chem. Eur. J.*, 1996, **2**, 1335.
6 R. J. H. Hafkamp, M. C. Feiters and R. J. M. Nolte, *Angew. Chem.*, 1994, **106**, 1054.
7 (*a*) N. A. J. M. Sommerdijk, P. J. J. A. Buynsters, A. M. A. Pistorius, M. Wang, M. C. Feiters, R. J. M. Nolte and B. Zwanenburg, *J. Chem. Soc., Chem. Commun.*, 1994, 1941; (*b*) N. A. J. M. Sommerdijk, P. J. J. A. Buynsters, A. M. A. Pistorius, M. Wang, M. C. Feiters, R. J. M. Nolte and B. Zwanenburg, *J. Chem. Soc., Chem. Commun.*, 1994, 2739; (*c*) N. A. J. M. Sommerdijk, M. H. L. Lambermon, M. C. Feiters, R. J. M. Nolte and B. Zwanenburg, *Chem. Commun.*, 1997, 455; (*d*) N. A. J. M. Sommerdijk, M. H. L. Lambermon, M. C. Feiters, R. J. M. Nolte and B. Zwanenburg, *Chem. Commun.*, 1997, 1423; (*e*) N. A. J. M. Sommerdijk, P. J. J. A. Buynsters, H. Akdemir, D. G. Geurts, A. M. A. Pistorius, M. C. Feiters, R. J. M. Nolte and B. Zwanenburg, *Chem. Eur. J.*, 1998, **1**, 127; (*f*) M. C. Feiters and R. J. M. Nolte, *Adv. Supramol. Chem.*, 2000, **6**, 41.
8 G. A. Ozin, *Acc. Chem. Res.*, 1997, **30**, 17.
9 (*a*) C. T. Kresge, M. E. Leonowicz, W. J. Roth, J. C. Vartuli and J. S. Beck, *Nature*, 1992, **359**, 710; (*b*) J. S. Beck, J. C. Vartuli, W. J. Roth, M. E. Leonowicz, C. T. Kresge, K. D. Schmitt, C. T. W. Chu, D. H. Olson, E. W. Sheppard, S. B. McCullen, J. B. Higgins and J. L. Schlenker, *J. Am. Chem. Soc.*, 1992, **114**, 10834.
10 (*a*) J. P. Spatz, S. Mößmer and M. Möller, *Chem. Eur. J.*, 1996, **2**, 1552; (*b*) M. Möller and J. P. Spatz, *Curr. Opin. Colloid Interface Sci.*, 1997, **2**, 177.
11 (*a*) S. Rajam, B. R. Heywood, J. B. A. Walker, S. Mann, R. J. Davey and J. D. Birchall, *J. Chem. Soc., Faraday Trans.*, 1991, **87**, 727; (*b*) B. R. Heywood and S. Mann, *Chem. Mater.*, 1994, **6**, 311.
12 (*a*) A. Wenzel and M. Antonietti, *Adv. Mater.*, 1997, **9**, 487; (*b*) M. Antonietti and C. Göltner, *Angew. Chem., Int. Ed. Engl.*, 1997, **36**, 910.
13 M. C. Feiters, in *Comprehensive Supramolecular Chemistry*, ed. J. L. Atwood, J. E. D. Davies, D. D. Macnicol and F. Vögtle, J. M. Lehn (Series editor), *Supramolecular Catalysis*, **vol. 10**, Pergamon, London, 1996.
14 J. M. Boggs, *Biochem. Biophys. Acta*, 1987, **906**, 353.
15 (*a*) J. G. H. Willems, M. C. Hersmis, R. de Gelder, J. M. M. Smits, J. B. Hammink, F. J. Dommerholt, L. Thijs and B. Zwanenburg, *J. Chem. Soc., Perkin Trans. 1*, 1997, 963; (*b*) J. G. H. Willems, J. B. Hammink, A. M. Vaarhorst, F. J. Dommerholt and B. Zwanenburg, *Tetrahedron Lett.*, 1995, **36**, 603 (the crystal structure determination and the crystallographic data will be published elsewhere); (*c*) N. A. J. M. Sommerdijk, P. J. J. A. Buynsters, H. Akdemir, D. G. Geurts, M. C. Feiters, R. J. M. Nolte and B. Zwanenburg, *J. Org. Chem.*, 1997, **62**, 4955.
16 (*a*) R. Mathis, R. Martino and A. Lattes, *Spectrochim. Acta, Part A*, 1974, **30**, 713 and references cited therein; (*b*) R. Mathis, R. Martino, F. Imberlin and A. Lattes, *Spectrochim. Acta, Part A*, 1974, **30**, 741.
17 G. A. Jeffrey, *Acc. Chem. Res.*, 1986, **19**, 168.
18 (*a*) H. A. Van Doren, T. J. Buma, R. M. Kellog and H. Wynberg, *J. Chem. Soc., Chem. Commun.*, 1988, 461; (*b*) H. A. Van Doren, R. Van der Geest, C. A. Keuning, R. M Kellog and H. Wynberg, *Liq. Cryst.*, 1989, **5**, 265.
19 R. A. Kühnel and S. J. van der Gaast, *Adv. X-Ray Anal.*, 1993, **36**, 439.
20 (*a*) The spherulites show a characteristic pattern (Maltese cross) under cross polarization, which may be similar to the patterns commonly observed in the smectic phase of liquid crystals see *e.g.* G. W. Gray and J. W. Goodby, *Smectic Liquid Crystals*, Leonard Hill, Philadelphia, 1984, pp. 9–17; (*b*) Recently a "spherular crystal" was observed when an amphiphilic single chain azacrown ether crystallized from its melt (see ref. 20*c*). This spherular crystal or spherulite has hierarchical structures: it consists of solid cylinders, and the cylinders are composed of the bilayers of the amphiphilic molecules; (*c*) R. Tang and Z. Tai, *Chem. Mater.*, 1998, **10**, 1638.
21 A. R. H. Cole and P. R. Jefferies, *J. Chem. Soc.*, 1956, 4391.
22 (*a*) C. G. Cannon, *Spectrochim. Acta*, 1958, **10**, 341; (*b*) S. N. Vinogradov and R. H. Linnell, *Hydrogen Bonding*, 1st edn., Litton Educational Publishing Inc., New York, 1971, ch. 3, p. 47; (*c*) L. J. Bellamy, *The Infra-red Spectra of Complex Molecules*, 3rd edn., Chapman and Hall Ltd., London, 1975, ch. 6, p. 107.
23 (*a*) R. G. Snyder, *J. Mol. Spectrosc.*, 1961, **7**, 161; (*b*) R. G. Snyder, *J. Chem. Phys.*, 1961, **47**, 1316; (*c*) R. G. Snyder and J. H. Schaachtschneider, *Spectrochim. Acta*, 1963, **19**, 85; (*d*) R. A. MacPhail, H. L. Strauss, R. G. Snyder and C. A. Elliger, *J. Chem. Phys.*, 1982, **88**, 334; (*e*) N. Yamada, K. Okuyama, M. Serizawa, M. Kawasaki and S. Oshima, *J. Chem. Soc., Perkin Trans. 2*, 1996, 2707; (*f*) N. Garti and K. Sato, *Crystallization and Polymorphism of Fats and Fatty Acids*, 1st edn., Marcel Dekker, 1988, ch. 4, p. 139; (*g*) A. N. Parikh, M. A. Schivley, E. Koo, K. Seshadri, D. Aurentz, K. Mueller and D. L. Allara, *J. Am. Chem. Soc.*, 1997, **119**, 3135.
24 (*a*) L. P. Kuhn, *J. Am. Chem. Soc.*, 1951, **74**, 2492; (*b*) L. P. Kuhn, *J. Am. Chem. Soc.*, 1954, **76**, 4323.
25 A. Baker, J. P. Davies and B. Gaunt, *J. Chem. Soc.*, 1949, 24.
26 (*a*) N. D. Coggeshall, *J. Am. Chem. Soc.*, 1947, **69**, 1620; (*b*) R. A. Riedel, *J. Am. Chem. Soc.*, 1951, **73**, 2881; (*c*) F. A. Smith and E. C. Creitz, *J. Res. Natl. Bur. Stand. (U. S.)*, 1951, **46**, 145.

27 In general, the frequency shift of an intramolecular hydrogen bond is less pronounced than for intermolecular hydrogen bonding, see ref. 22.
28 The enhanced degree of order after reorganisation of the molecules was confirmed by powder diffraction experiments, which showed an increase in the number of peaks as well as a sharpening. However, a sub-cell structure has not yet been deduced from these complicated diffractograms.
29 The pK_a^* values of **1b, c** in methanol–water (95 : 5; v/v) were determined by potentiometric titration and amounted to 8.5. Hence, it may be assumed that in water adjusted to pH 3.0 the molecules are protonated.
30 (*a*) D. Hönig and D. Möbius, *J. Phys. Chem.*, 1991, **62**, 4590; (*b*) S. Hénon and J. Meunier, *Rev. Sci. Instrum.*, 1991, **62**, 936.
31 The dimensions of the condensed phase domains of **1c** are in the sub-microscopic scale (<1–2 μm) and therefore cannot be detected with BAM, see *e.g.* D. Vollhardt, *Adv. Colloid Interface Sci.*, 1999, **79**, 19.
32 Aggregate morphology can be manipulated by the addition of different counter ions or organic solutes, see *e.g.* refs. 7*c–e* and (*a*) T. Tachibana and H. Kambara, *Bull. Chem. Soc. Jpn.*, 1969, **42**, 3422; (*b*) T. Tachibana, S. Kitazawa and H. Takeno, *Bull. Chem. Soc. Jpn.*, 1970, **43**, 2418; (*c*) N. A. Mazer and G. Olofson, *J. Phys. Chem.*, 1982, **86**, 4584; (*d*) T. Kunitake, J.-M. Kim and Y. Ishikawa, *J. Chem. Soc., Perkin Trans. 2*, 1991, 885; (*e*) T. M. Claussen, P. K. Vinson, J. R. Minter, H. T. Davis, Y. Talmon and W. G. Miller, *J. Phys. Chem.*, 1992, **96**, 474; (*f*) N. Yamada, M. Iijima, K. Vongbupnimit, K. Noguchi and K. Okuyama, *Angew. Chem., Int. Ed.*, 1999, **38**, 91.
33 H. Hoffmann and G. Ebert, *Angew Chem., Int. Ed. Engl.*, 1988, **27**, 902.
34 (*a*) Y. Saikaigudin, T. Shikahata, H. Urakami, A. Tamura and H. Hirata, *J. Electron Microsc.*, 1987, **36**, 168; (*b*) H. Hitata and Y. Saikaigudin, *Bull. Chem. Soc. Jpn.*, 1989, **62**, 581.
35 Other organic counter ions, *e.g.* oxalate, maleate and phthalate also did not lead to any distinct aggregate morphologies.